Chapter 5

Orthogonal control of antibacterial activity with light

***Published in*: ACS Chemical Biology 2014 Sep 19;9(9):1969-74**

Willem A. Velema[a], Jan Pieter van der Berg[b],Wiktor Szymanski[a], Arnold J. M. Driessen[b,c] & Ben L. Feringa[a,c]

[a]Centre for Systems Chemistry, Stratingh Institute for Chemistry, University of Groningen, Groningen, The Netherlands.

[b]Molecular Microbiology, Groningen Biomolecular Sciences and Biotechnology Institute, University of Groningen, Groningen, The Netherlands.

[c]Zernike Institute for Advanced Materials, University of Groningen, Groningen, The Netherlands.

Abstract

Selection of a single bacterial strain out of a mixture of microorganisms is of crucial importance in healthcare and microbiology research. Novel approaches that can externally control bacterial selection are a valuable addition to the microbiology toolbox. In this proof-of-concept, two complementary antibiotics are protected with photocleavable groups that can be orthogonally addressed with different wavelengths of light. This allows for the light-triggered selection of a single bacterial strain out of a mixture of multiple strains, by choosing the right wavelength. Further improvement toward additional orthogonally-addressable antibiotics might ultimately lead to a novel methodology for bacterial selection in complex populations.

Introduction

Microorganisms are able to co-exist in mixed populations, which can cause complex bacterial infections, i.e. infections with two or more unrelated strains, and what can also be a source of sample infections in microbiology practice [1]. Specifically addressing a single bacterial strain [2,3] from a mixture of multiple strains is a fascinating scientific challenge and a necessity in healthcare for diagnostics and screening and provides an important tool in microbiology research [4].

Of special interest are methods that attain bacterial selection using an external trigger, with minimal perturbation to the studied microbial population. Furthermore, it would be advantageous if this trigger could be delivered with high spatiotemporal precision, as it not only allows for externally controlled bacterial selection, but it might be exploited for precise bacterial patterning as well [5,6].

The use of light as an external trigger to control biological processes, such as cellular growth, is an interesting option, since the delivery of light can be precisely controlled in space and time. Additionally, light is relatively non-invasive and bioorthogonal and it does not cause sample contamination [7–12]. Furthermore, both the qualitative (wavelength) and quantitative (amplitude) properties of light can be precisely controlled, allowing independent and regulated activation of several species [13].

Significant progress has been made in achieving optical control over biological processes [14] using photoisomerisable moieties [8,15,16]. Recent examples include the remote control of protein channel function [17], nociception regulators [18], enzyme inhibitors [19,20], mast cell activation inhibitors [21] and antibiotics [5]. However, in all these cases only a single process was targeted. To develop a system for bacterial selection it is necessary to address the activity of multiple antimicrobial agents separately. Photocontrol over multiple events in parallel has recently been shown for functional

surfaces [22], protein kinase activation [23], and photodeprotection of oligonucleotides [13]. Remarkable reports of selective photochemical control [24,25] include glutamate and GABA uncaging [26,27] and photoinitiation and -inhibition for photolithography [28]. Using various photocleavable protecting groups [29–31], with a significant difference in λ_{max}, allows for the control of multiple processes in an orthogonal fashion. Various photocleavable protecting groups are available, such as *ortho*-nitrobenzyl groups, coumarins and arylcarbonylmethyl groups [29–32].

Here we describe a proof-of-concept for the orthogonal photocontrol over bacterial growth. First, the design of two antibiotics with orthogonally phototriggered activity is discussed, regarding their photochemical and antimicrobial properties in response to irradiation. Subsequently, analysis of the photochemistry of the two caged antibiotics is described. The antibacterial properties of the designed compounds were determined before and after photo-activation, for *Escherichia coli* and *Staphylococcus aureus*. Finally, the orthogonal release of antimicrobial substances is used for bacterial selection. This system can be triggered by two different wavelengths, where the absence or presence of light at these wavelengths induces selective growth of *E. coli* and *S. aureus*. Within this proof-of-concept, we report on the selection of either one bacterial strain out of a mixture of two. However, rapid advances in the field of photochemistry and the vastly growing number of orthogonally addressable photocleavable groups, will likely extend this method to be applicable for bacterial selection out of more complex mixtures of microorganisms.

Results and Discussion

When designing a system that allows for orthogonally controlling bacterial growth, several factors need to be taken into account. Firstly, two antibiotics should be chosen, that are complementary in their antibacterial spectrum, i.e. when using a mixture of two bacteria, the first antibiotic inhibits the growth of only one bacterium but does not affect the growth of the other and the second antibiotic does the opposite. A second consideration is the ease by which the antibiotics can be caged with a photolysable group. Carboxylic acid moieties present in the antimicrobial agents are especially suitable for this purpose. Furthermore, the protected antibiotics must show significantly lower activity when compared to the native ones. Another prerequisite is sufficient water solubility of the designed compounds. When all these design elements are combined, a system can be assembled as schematically depicted in Figure 1.

Based on the above-mentioned considerations, a fluoroquinolone **(1)** and benzylpenicillin **(2)** were selected as antibiotics (Fig. 2a). The two bacteria chosen for this

system were *E. coli* and *S. aureus*. *E. coli* is susceptible to the fluoroquinolone **(1)**, but is not affected by benzylpenicillin **(2)**, whereas *S. aureus* is sensitive for **2**, but is not affected by the fluoroquinolone (*vide infra*). Additionally, both antibiotics bear a carboxylic acid functionality, which can be protected with a photolysable group. The carboxylic group of fluoroquinolones is essential for binding to DNA bases [33] and caging of this group would result in significant loss of activity, which would be regained after photolysis. The carboxylate group of compound **2** interacts with the binding site of transpeptidase [34] and its modification into a photolysable-ester reduces the antimicrobial activity, which can be restored after photodeprotection.

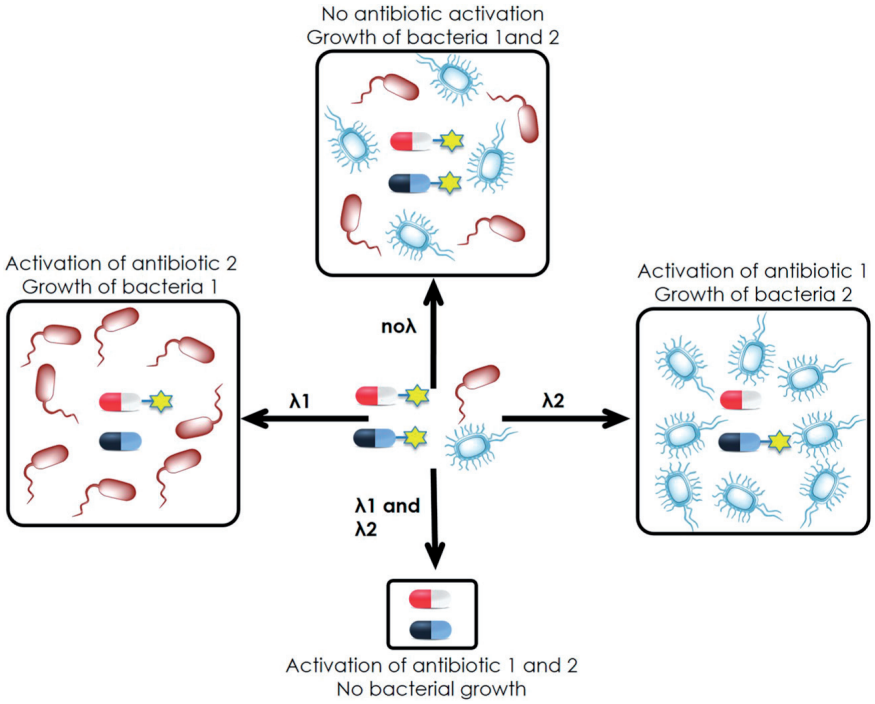

Figure 1 Schematic representation of the required elements for light-triggered bacterial selection. Two complementary antibiotics that can be orthogonally activated with different wavelengths of light are combined with two different bacteria. Activation of antibiotic 1 causes a growth inhibition of bacteria 1 and results in growth of bacteria 2. When antibiotic 2 is activated, the growth of bacteria 2 is inhibited and growth of bacteria 1 is realized. When none of the antibiotics is activated, bacteria 1 and bacteria 2 will grow. Activation of both antibiotics leads to death of both bacteria.

Derivatives of 7-dialkylaminocoumarin and 7-alkoxycoumarin were used as photo-cleavable groups. These compounds show absorption bands with a λ_{max} of ~380 nm and ~310 nm, respectively, which allows for orthogonal photo-activation. Furthermore, the amino and hydroxyl groups can be alkylated with carboxylic acid-bearing compounds, which renders these molecules water-soluble. The two designed photo-activatable antibiotics are shown in Figure 2a.

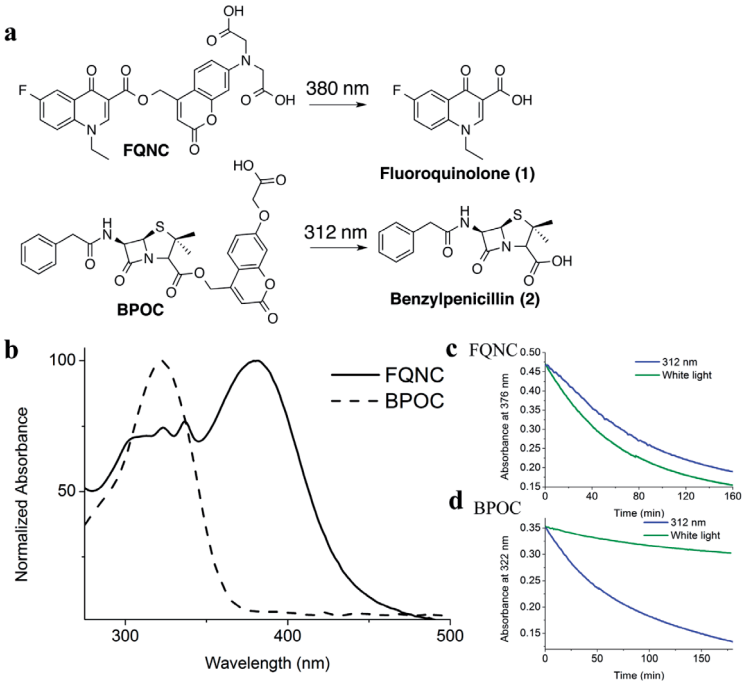

Figure 2 Molecular structure of designed photo-activatable antibiotics and products liberated after photocleavage and change in UV-Vis absorption spectra. a) **FQNC** consists of a fluoroquinolone which was protected at its carboxylic acid group with a derivative of 7-aminocoumarin. The coumarin moiety can be cleaved from **FQNC** by illumination with 380 nm light, liberating the free carboxylic acid functionality of the fluoroquinolone **(1)**. The molecular structure of **BPOC** comprises a benzylpenicillin, which was conjugated with a derivative of 7-hydroxycoumarin at its carboxylic moiety. Exposing **BPOC** to 312 nm light releases benzylpenicillin. b) The UV-Vis spectrum of **FQNC** shows an absorption maximum at 381 nm as well as significant absorbance between 300-350 nm. **BPOC** has one absorption band with a maximum around 320 nm. c) and d) The photocleavage of **FQNC** (25 μM in water) and **BPOC** (18 μM in water) was measured over time by observing the decrease in absorbance at λ_{max} (381 nm and 322 nm, respectively) using UV-Vis spectroscopy.

The fluoroquinolone analog was named **FQNC** (FluoroQuinolone-*N*-Coumarin) (Fig. 2a) and was protected with a disubstituted 7-aminocoumarin group, which allows for photo-activation at 380 nm (*vide infra*). The photoactivatable benzylpenicillin (Fig. 2a) bears a substituted 7- hydroxycoumarin moiety which could be released by irradiation with 312 nm light (*vide infra*). This compound was named **BPOC** (BenzylPenicillin-*O*-Coumarin).

UV-Vis spectroscopy was used to study the photochemical properties of the photoactivatable antibiotics. An absorption-band for **FQNC** with a λ_{max} of 381 nm was observed (Fig. 2b). Irradiation with white light resulted in a decrease of this absorption-band, indicating that the photolysable coumarin group was cleaved and **1** was liberated. **BPOC** has an absorption maximum at 322 nm (Fig. 2b). When this sample was illuminated with 312 nm light, a decrease in absorption was observed. This decrease is caused by the photodeprotection of **BPOC**, which results in the release of benzylpenicillin **2**. To examine the orthogonality of this photocleavage process, the rate of photodeprotection was studied for **FQNC** and **BPOC** with 312 nm and white light irradiation (Fig. 2c and 2d), by observing the decrease in absorption at λ_{max}. Figure 2c shows that **FQNC** could be deprotected by irradiation with white light (150W, 1 cm distance, see Fig. S1 for spectrum). Illuminating a sample with 312 nm light (8W, 2 cm distance) also resulted in complete deprotection. This might be caused by a strong absorption of the quinolone moiety at these wavelengths, which may result in energy transfer, preventing selective deprotection of **FQNC** by white light only. However, **FQNC** and **BPOC** have a large difference in antibacterial activity and exploiting these properties results in orthogonal growth of *E. coli* and *S. aureus* (*vide infra*). The photodeprotection rate was also studied for **BPOC** (Fig. 2d). When **BPOC** was exposed to white light, only a small decrease in absorption was observed, whereas a much more dramatic decrease in absorption was achieved using 312 nm light irradiation. This enables selective activation of **BPOC** with UV light. To further confirm the liberation of **1** from **FQNC** and **2** from **BPOC** after exposure to light, ^{1}H NMR spectroscopy and HR-MS were used to characterize the deprotected antibiotics (Fig. S2-S4). The quantum yields of **FQNC** and **BPOC** were determined to be 7.2 x 10^{-4} (at 323 nm) and 8.9 x 10^{-3} (at 376 nm), respectively. Furthermore, the compounds were stable for at least 4 h when dissolved in water (Fig. S5-S6).

FQNC and **BPOC** are the carboxyl-protected analogs of **1** and **2**, respectively. The bacteria used for this study were *E. coli* CS1562 (*tolC6*::*tn10*) [35] and *S. aureus* RN4220 [36]. Compound **1** has antibacterial activity against *E. coli* with a minimal inhibitory concentration (MIC) (lowest concentration that still inhibits bacterial growth) of 68

μM (Fig. 3a and Fig. S7) and has significantly lower activity against *S. aureus* with a MIC of >1700 μM (Fig. 3a and Fig. S7). In contrast, **2** has high activity against *S. aureus* with a MIC of 350 nM (Fig. 3a and Fig. S8) and dramatically less activity against *E. coli* with a MIC of 288 μM (Fig. 3a and Fig. S8). Figure 3b shows bacterial growth curves of *E. coli* when incubated with 76 μM of **FQNC**, before and after exposure to white light (See Fig. S9 for MIC determination of **FQNC**). Before exposure to white light, normal bacterial growth was observed, comparable to the control without any antibiotic present. After irradiating the samples for 5 min with white light, bacterial growth was inhibited. This indicates that **1** was liberated after white light exposure, inhibiting bacterial growth.

a

Compound	MIC *E. coli* (μM)	MIC *S. aureus* (μM)
1	68	>1700
2	288	0.35

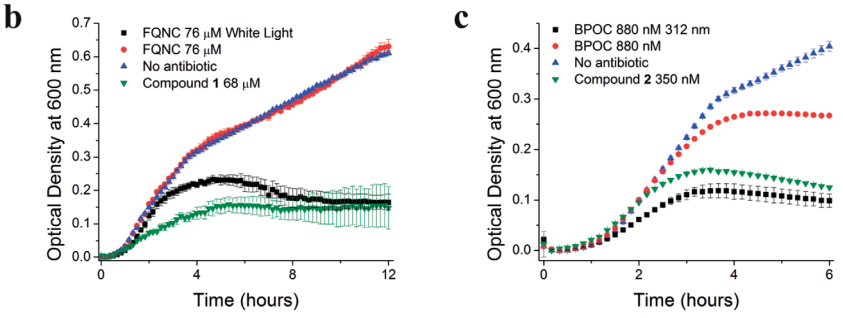

Figure 3 MIC values and bacterial growth curves of *E. coli* and *S. aureus* incubated with **FQNC** and **BPOC** before and after photodeprotection. a) MIC values of compounds **(1)** and **(2)**. b) When *E. coli* was incubated with 76 μM of **FQNC** it exhibited a normal growth pattern comparable with the control without **FQNC**. When the samples were exposed to white light prior to incubation, *E. coli* growth was inhibited. c) The growth of *S. aureus* was significantly inhibited when incubated with 880 nM **BPOC** which was irradiated at 312 nm, as compared to *S. aureus* that was incubated with 880 nM **BPOC** which had not been exposed to light. Error bars show standard deviations calculated from measurements in triplicate.

Next, a similar experiment was conducted for **BPOC**. Samples of **BPOC** (880 nM) that were exposed to 312 nm for 2 min, prior to incubation with *S. aureus*, showed minimal bacterial growth (Fig. 3c). When *S. aureus* was incubated with samples with the same concentration of **BPOC** but without exposure to light, significantly more

bacterial growth was observed. The MIC of **BPOC** against *S. aureus* was 3.5 μM without exposure (Fig. S9) and 880 nM with exposure to 312 nm light. These experiments indicate that the antibiotic activity of the two protected compounds **FQNC** and **BPOC** can be induced at two distinct different wavelengths. Furthermore, the liberated antibiotics show a large difference in spectrum of activity, as was expected, and therefore inhibit bacterial growth of different bacterial strains. This is an important prerequisite for realizing our system for bacterial selection. By combining these properties, **FQNC** and **BPOC** can be employed for light-triggered bacterial selection. To realize this, agar-plates were prepared, that contained 48 μM **FQNC** and 350 nM **BPOC**. Next, the agar-plates were kept in the dark or exposed to 312 nm light (10 sec), white light (5 min), or both 312 nm and white light. Subsequently, the plates were divided in three equal parts (Fig. 4a). One part was inoculated with *E. coli* ('*E. coli*' sector), another part with *S. aureus* ('*S. aureus*' sector) and the third part was inoculated with both bacteria ('both' sector). After incubation overnight, (the lack of) bacterial growth could be observed (Fig. 4a). The plate (P1) that was not exposed to any light showed bacterial growth in all three sectors, indicating that *E. coli*, as well as *S. aureus*, were growing. When closely examining the colonies, a distinct difference in morphology between the colonies of *E. coli* and *S. aureus* could be observed (Fig. 4b). At the 'both' sector both morphologies were present (Fig. 4b). The second plate (P2) that was exposed to 312 nm light showed no growth at the *S. aureus* sector and normal growth at the other two sectors which implies that only *E. coli* was growing which was also evident from the colony morphology. The third plate (P3) was exposed to white light and did not show any growth at the *E. coli* sector whereas normal growth was observed in the other two sectors. This suggests that only *S. aureus* was growing also evidenced by colony morphology The last plate (P4) was exposed to 312 nm and white light and after incubating overnight, almost no bacterial growth was observed in any of the sectors, indicating that *E. coli* as well as *S. aureus* growth was inhibited. These observations prove that **FQNC** and **BPOC** can be employed to select each of the bacterial strains out of a mixture of two strains. This proof-of-concept shows that light can be used as an external trigger to control bacterial selection. This concept holds promise to be expanded to a larger number of orthogonally activated antibiotics, which will allow for bacterial selection from more complex mixtures of microorganisms, using light. Such future studies will be supported by the rapid advancement in the design of orthogonally addressable photocleavable groups. Complex mixtures of various bacterial strains might be analyzed and cell populations selected, by simply exposing the system to the right wavelengths

of irradiation. The methodology presented here represents a valuable addition to the toolbox for bacterial selection and might also be particular useful for high-precision patterning of various microorganisms in one system.

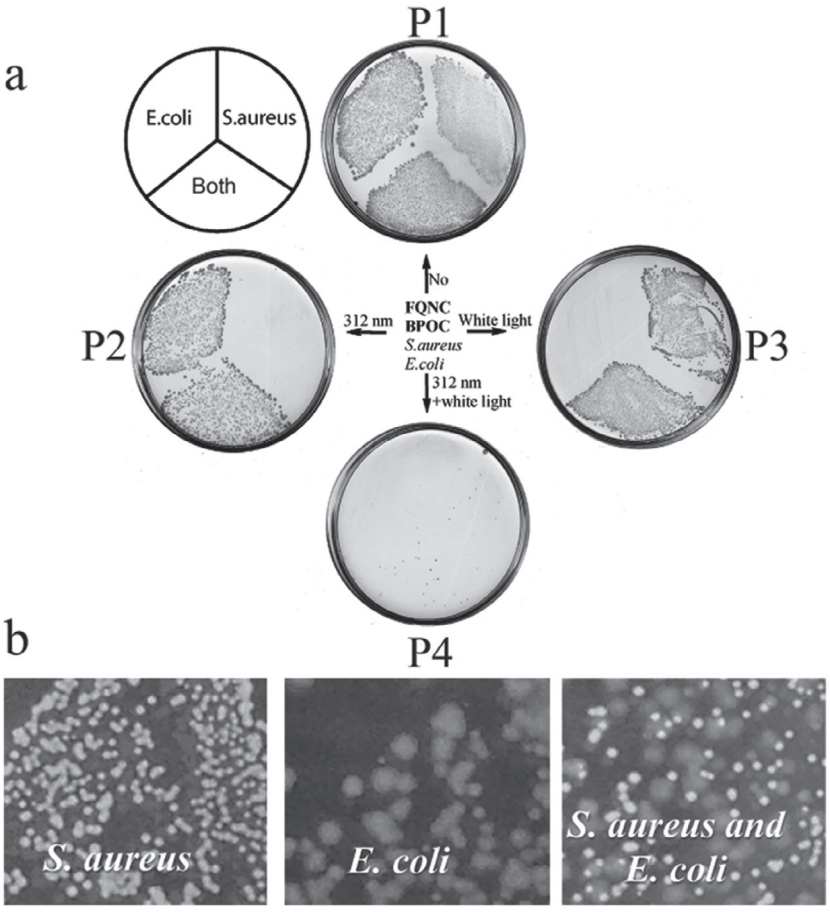

Figure 4 Light-triggered bacterial selection. a) Agar-plates containing **FQNC** (48 μM) and **BPOC** (350 nM) were kept in the dark or exposed to 312 nm light, white light or a combination of 312 nm light and white light. Subsequently, *E. coli* and *S. aureus* were inoculated at different sectors on the plate. Overnight incubation resulted in bacterial growth in selected sectors on the agar-plates. b) A close-up of the colonies formed by *E. coli* and *S. aureus.* There was a distinct difference in morphology of colonies of the two bacterial strains. When the two bacteria were grown together with and without the photoactivatable antibiotics, the two different morphologies were distinguishable.

Methods

Synthesis of FQNC and BPOC

The synthesis of **FQNC** and **BPOC** is described in the supplementary information.

Uncaging Experiments

Irradiation experiments were performed with a Spectroline ENB-280C/FE UV lamp (312 nm) and Thor Labs OSL1-EC Fiber Illuminator (white light) (see Fig S1 for lam emission spectrum).

Quantum Yield Determination

Quantum yields were determined by irradiating 2.5 μM solutions of **BPOC** and **FQNC** with 323 nm and 376 nm light, respectively, with a JASCO FP-6200 spectrofluorometer. After each irradiation period UV-Vis absorbance was measured. The percentage of photolysis was estimated by the decrease in absorbance at λ_{max}. Quantum yields (Q) of photolysis were calculated using the following equation: $Q = -\log(C_t/C_0)/(I\sigma t)$. C_t and C_0 are the concentrations of **BPOC** or **FQNC** at time t and time 0 respectively. σ is the decadic extinction coefficient in $cm^2 \cdot mol^{-1}$, t is the irradiation time in seconds and I is the light intensity in $einsteins \cdot cm^{-2} \cdot s^{-1}$ that was determined using ferrioxalate actinometry [37].

Bacterial strains and growth conditions

The bacterial strains used were *E. coli* CS1562 (*tolC6*:*tn10*) [35] and *S. aureus* RN4220 [36]. Both strains were grown in LB medium (5 g/L yeast extract; 10 g/L tryptone; 0.5 g/L NaCl) supplemented with the required antibiotic at 37 °C.

Solid medium

An LB agar plate containing **FQNC** and **BPOC** was not irradiated with light, irradiated with UV light for 10 sec and/or visible light for 5 min. The plate was then streaked with approximately 10^4 CFUs of *E. coli* CS1562 and *S. aureus* RN4220 and incubated overnight at 37 °C.

Antibacterial activity and bacterial growth curves

Overnight cultures of *E. coli* CS1562 and *S. aureus* RN4220 were diluted to an OD_{600} of 0.1 and 100 μl of this cell suspension was added to 100 μl medium containing antibiotics at the given concentration. To determine the antibacterial activity after light

exposure, the solutions were first irradiated at 312 nm for 2 min or white light for 5 min prior to adding the cell suspension. Cells were grown in a microtiter plate at 37 °C and cell density (OD at 600 nm) was measured every 10 min for 12 h, with a 10 sec shaking step before each measurement, in a microplate reader (SynergyMX, BioTek). Graphs were background-corrected by subtracting the OD_{600} at time 0. Before calculating the growth rate, graphs were plotted on a logarithmic scale. Growth rates were determined by calculating the slope of the exponential growth phase. MIC values were calculated by plotting the growth rates against the concentrations of the used antibiotics.

Associated content

Supporting Information Additional figures and synthetic procedures are available free of charge via the internet at http://pubs.acs.org.

Acknowledgements

This work was financially supported by the Netherlands Organization for Scientific Research (NWO-CW), The Royal Netherlands Academy of Arts and Sciences Science (KNAW) and the European Research Council (ERC) advanced grant 227897 to B.L.F.) and the Ministry of Education, Culture and Science (Gravity programme no. 024.001.035).

References

1. Tyre, D. W. *et al.* Detection of Mixed Infection from Bacterial Whole Genome Sequence Data Allows Assessment of Its Role in *Clostridium difficile* Transmission. *PLoS Comput. Biol.* **9**, e1003059 (2013).
2. Ngo, J. T. *et al.* Cellselective metabolic labeling of proteins. *Nat. Chem. Biol.* **5**, 715–717 (2009).
3. Truong, F., Yoo, T. H., Lampo, T. J., and Tirrell, D. A. Two-strain, cellselective protein labeling in mixed bacterial cultures. *J. Am. Chem. Soc.* **134**, 8551–6 (2012).
4. Gomaa, A. A. *et al.* Programmable Removal of Bacterial Strains by Use of Genome-Targeting CRISPR-Cas Systems. *mBio* **5**, e00928–13 (2013).
5. Velema, W. A. *et al.* Optical control of antibacterial activity. *Nat. Chem.* **5**, 924–928 (2013).
6. Babii, O. *et al.* Controlling Biological Activity with Light: Diarylethene-Containing Cyclic Peptidomimetics. *Angew. Chemie Int. Ed.* **53**, 3392–3395 (2014).
7. Mayer, G., and Heckel, A. Biologically active molecules with a "lightswitch". *Angew. Chem. Int. Ed.* **45**, 4900–4921 (2006).

8. Szymanski, W., Beierle, J. M., Kistemaker, H. A. V, Velema, W. A., and Feringa, B. L. Reversible photocontrol of biological systems by the incorporation of molecular photoswitches. *Chem. Rev.* **113**, 6114–6178 (2013).
9. Velema, W. A., Szymanski, W., and Feringa, B. L. Photopharmacology: beyond proof of principle. *J. Am. Chem. Soc.* **136**, 2178–91 (2014).
10. Gorostiza, P., and Isacoff, E. Y. Optical switches for remote and noninvasive control of cell signaling. *Science* **322**, 395–399 (2008).
11. Mbatia, H. W., and Burdette, S. C. Photochemical tools for studyingmetal ion signaling and homeostasis. *Biochemistry* **51**, 7212–24 (2012).
12. Bandara, H. M. D., and Burdette, S. C. Photoisomerization in differentclasses of azobenzene. *Chem. Soc. Rev.* **41**, 1809 (2012).
13. Rodrigues-Correia, A., Weyel, X. M. M., and Heckel, A. Four Levels of Wavelength-Selective Uncaging for Oligonucleotides. *Org. Lett.* **15**, 5500–5503 (2013).
14. Deisseroth, K. Optogenetics. *Nat. Methods* **8**, 26–29 (2011).
15. Mourot, A., Tochitsky, I., and Kramer, R. H. Light at the end of the channel: optical manipulation of intrinsic neuronal excitability with chemical photoswitches. *Front. Mol. Neurosci.* **6**, 5 (2013).
16. Beharry, A. B., and Woolley, G. A. Azobenzene photoswitches for biomolecules. *Chem. Soc. Rev.* **40**, 4422–4437 (2011).
17. Kocer, A., Walko, M., Meijberg, W., and Feringa, B. L. A light-actuated nanovalve derived from a channel protein. *Science* **309**, 755–758 (2005).
18. Mourot, A. *et al.* Rapid optical control of nociception with an ion-channel photoswitch. *Nat. Methods* **9**, 396–402 (2012).
19. Vomasta, D., Högner, C., Branda, N. R., and König, B. Regulation of human carbonic anhydrase I (hCAI) activity by using a photochromic inhibitor. *Angew. Chem. Int. Ed. Engl.* **47**, 7644–7647 (2008).
20. Chen, X. *et al.* Acetylcholinesterase Inhibitors with Photoswitchable Inhibition of β-Amyloid Aggregation. *ACS Chem. Neurosci.* **5**, 377-389 (2014).
21. Velema, W. A., van der Toorn, M., Szymanski, W., and Feringa, B. L. Design, Synthesis, and Inhibitory Activity of Potent, Photoswitchable Mast Cell Activation Inhibitors. *J. Med. Chem.* **56**, 4456–4464 (2013).
22. San Miguel, V., Bochet, C. G., and del Campo, A. Wavelength-Selective Caged Surfaces: How Many Functional Levels Are Possible? *J. Am. Chem. Soc.* **133**, 5380–5388 (2011).
23. Priestman, M. A., Sun, L., and Lawrence, D. S. Dual Wavelength Photoactivation

of cAMP- and cGMP-Dependent Protein Kinase Signaling Pathways. *ACS Chem. Biol.* **6**, 377–384 (2011).
24. Fournier, L. *et al.* A blue-absorbing photolabile protecting group for in vivochromatically orthogonal photoactivation. *ACS Chem. Biol.* **8**, 1528–1536 (2013).
25. Fournier, L. *et al.* Coumarinylmethyl caging groups with redshifted absorption. Chem. - Eur. J. **19**, 17494–17507 (2013).
26. Kantevari, S., Matsuzaki, M., Kanemoto, Y., Kasai, H., and Ellis-Davies, G. C. R. Two-color, two-photon uncaging of glutamate and GABA. *Nat. Methods* **7**, 123–125 (2010).
27. Amatrudo, J. M. *et al.* Wavelength-selective one- and two-photon uncaging of GABA. *ACS Chem. Neurosci.* **5**, 64–70 (2014).
28. Scott, T. F., Kowalski, B. A., Sullivan, A. C., Bowman, C. N., and McLeod, R. R. Two-color single-photon photoinitiation and photoinhibition for subdiffraction photolithography. *Science* **324**, 913–917 (2009).
29. Klán, P. *et al.* Photoremovable Protecting Groups in Chemistry and Biology: Reaction Mechanisms and Efficacy. *Chem. Rev.* **113**, 119–191 (2013).
30. Deiters, A. Principles and applications of the photochemical control of cellular processes. *Chembiochem.* **11**, 47–53 (2010).
31. Brieke, C., Rohrbach, F., Gottschalk, A., Mayer, G., and Heckel, A. Light-controlled tools. *Angew. Chem. Int. Ed. Engl.* **51**, 8446–76 (2012).
32. Wu, T., Tang, H., Bohne, C., and Branda, N. R. Reporting the release of caged species by a combination of two sequential photoreactions, a molecular switch, and one color of light. *Angew. Chem. Int. Ed. Engl.* **51**, 2741–4 (2012).
33. Tillotson, G. S. Quinolones: structure-activity relationships and futurepredictions. *J. Med. Microbiol.* **44**, 320–324 (1996).
34. Yocum, R. R., Rasmussen, J. R., and Strominger, J. L. The mechanism of action of penicillin. Penicillin acylates the active site of *Bacillus stearothermophilus* D-alanine carboxypeptidase. *J. Biol. Chem.* **255**, 3977–3986 (1980).
35. Austin, E. A., Graves, J. F., Hite, L. A., Parker, C. T., and Schnaitman, C. A. Genetic analysis of lipopolysaccharide core biosynthesis by *Escherichia coli* K-12: insertion mutagenesis of the *rfa* locus. *J. Bacteriol.* **172**, 5312–5325 (1990).
36. Kreiswirth, B. N. *et al.* The toxic shock syndrome exotoxin structural gene is not detectably transmitted by a prophage. *Nature* **305**, 709–712 (1983).
37. Hatchard, C. G., and Parker, C. A. A New Sensitive Chemical Actinometer. II. Potassium Ferrioxalate as a Standard Chemical Actinometer. *Proc. R. Soc. London. Ser. A* **235**, 518–536 (1956).

Supporting information

Materials and Methods

Uncaging Experiments

Irradiation experiments were performed with a Spectroline ENB-280C/FE UV lamp (312 nm) and Thor Labs OSL1-EC Fiber Illuminator (white light) (see Fig S1 for electromagnetic spectrum).

Quantum Yield Determination

Quantum yields were determined by irradiating 2.5 μM solutions of **BPOC** and **FQNC** with 323 nm and 376 nm light, respectively, with a JASCO FP-6200 spectrofluorometer. After each irradiation period UV-Vis absorbance was measured. The percentage of photolysis was estimated by the decrease in absorbance at λ_{max}. Quantum yields (Q) of photolysis were calculated using the following equation: $Q = -\log(C_t/C_0)/(I\sigma t)$. C_t and C_0 are the concentrations of **BPOC** or **FQNC** at time t and time 0 respectively. σ is the decadic extinction coefficient in $cm^2 \cdot mol^{-1}$, t is the irradiation time in seconds and I is the light intensity in einsteins$\cdot cm^{-2} \cdot s^{-1}$ that was determined using ferrioxalate actinometry [(1)].

Bacterial strains and growth conditions

The bacterial strains used were *E. coli* CS1562 (*tolC6*:*tn10*) [(2)] and *S. aureus* RN4220 [(3)]. Both strains were grown in LB medium (5 g/L yeast extract; 10 g/L tryptone; 0.5 g/L NaCl) supplemented with the required antibiotic at 37 °C.

Solid medium

An LB agar plate containing **FQNC** and **BPOC** was not irradiated, irradiated for 10 seconds with UV light and/or visible light for 5 min. The plate was then streaked with approximately 10^4 CFUs of *E. coli* CS1562 and *S. aureus* RN4220 and incubated overnight at 37 °C.

Antibacterial activity and bacterial growth curves

Overnight cultures of *E. coli* CS1562 and *S. aureus* RN4220 were diluted to an OD_{600} of 0.1 and 100 μl of this cell suspension was added to 100 μl medium containing antibiotics at the given concentration. To determine the antibacterial activity after light exposure, the solutions were first irradiated at 312 nm for 2 min or with white light for 5 min

prior to adding the cell suspension. Cells were grown in a microtiter plate at 37 °C and cell density (OD at 600 nm) was measured every 10 min for 12 h, with a 10 sec shaking step before each measurement, in a microplate reader (SynergyMX, BioTek). Graphs were background-corrected by subtracting the OD_{600} at time 0. Before calculating the growth rate, graphs were plotted on a logarithmic scale. Growth rates were determined by calculating the slope of the exponential growth phase. MIC values were calculated by plotting the growth rates against the concentrations of the used antibiotics.

Synthesis General

All chemicals for synthesis were obtained from commercial sources and used as received unless stated otherwise. Solvents were reagent grade. Thin-layer chromatography (TLC) was performed using commercial Kieselgel 60, F254 silica gel plates. Flash chromatography was performed on silica gel (Silicycle Siliaflash P60, 40-63 μ, 230-400 mesh). Drying of solutions was performed with $MgSO_4$ and solvents were removed with a rotary evaporator. Chemical shifts for NMR measurements were determined relative to the residual solvent peaks (δH 7.26 for $CHCl_3$ and 2.50 for DMSO, δC 77.16 for $CDCl_3$ and 39.52 for DMSO). The following abbreviations are used to indicate signal multiplicity: s, singlet; d, doublet; t, triplet; q, quartet; m, multiplet; brs, broad signal; appt, apparent triplet. HRMS (ESI) spectra were obtained on a Thermo scientific LTQ Orbitrap XL. Melting points were recorded using a Buchi melting point B-545 apparatus. UV/Vis absorption spectra were recorded on an Agilent 8453 UV-Visible Spectrophotometer using Uvasol grade solvents.

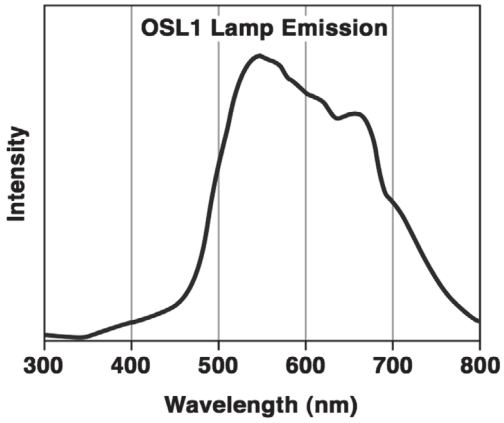

Figure S1 Electromagnetic spectrum of the white light source that was used for the white-light irradiation experiments (Thor Labs OSL1-EC Fiber Illuminator). *Source: www.thorlabs.de*

^{1}H NMR spectra of FQNC and BPOC after irradiation

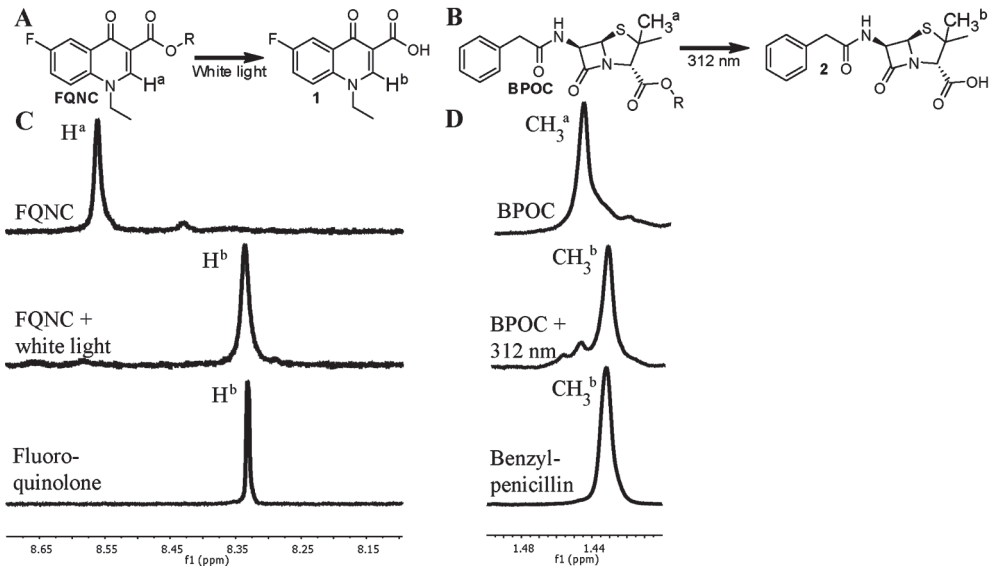

Figure S2 ^{1}H NMR spectroscopic confirmation of antibiotic release in D_2O (10 mM). a) The photodeprotection process of **FQNC** using white light, resulting in the liberation of **1**. The protons that are observed in C are denoted as H^a and H^b. b) The release of **2** from **BPOC** with 312 nm light. The protons that are observed in D are denoted as $CH_3{}^a$ and $CH_3{}^b$. c) H^a is observed as a singlet at 8.57 ppm; after **FQNC** was illuminated with white light for 30 h, this signal shifted to 8.34 ppm, which is similar to the shift of H^b in **1** which verifies the antibiotic release. d) $CH_3{}^a$ appears in the non-irradiated sample as a singlet at 1.45 ppm. Irradiation with 312 nm light caused this singlet to shift to 1.43 ppm, which is similar to the shift of $CH_3{}^b$ in **2**, confirming the liberation of the antibiotic.

HR-MS spectra of FQNC and BPOC after irradiation

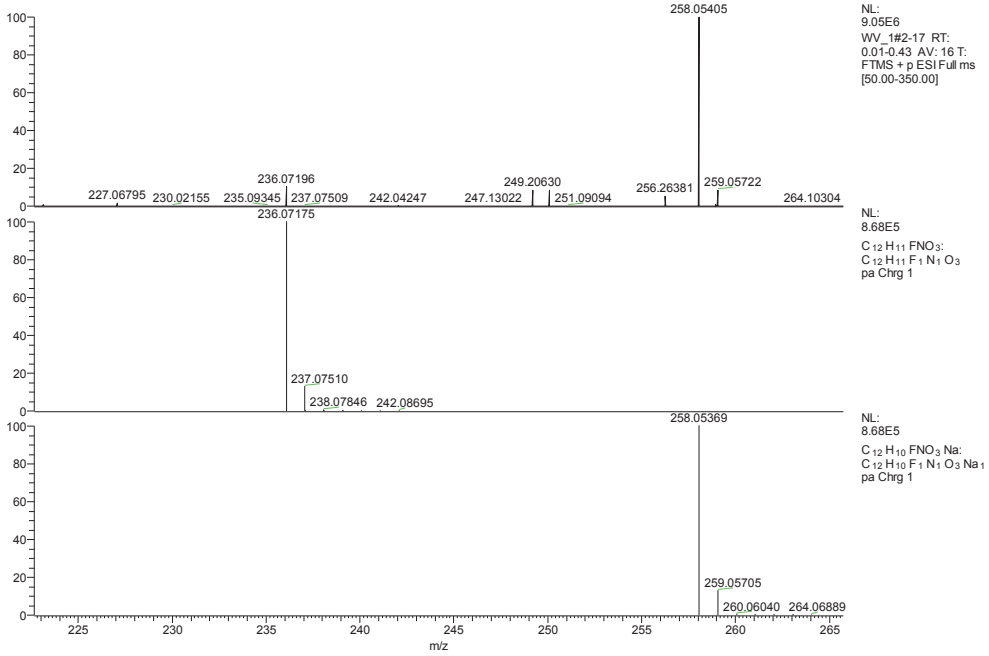

Figure S3 A saturated solution of **FQNC** in water was irradiated with visible light for 5 min. The obtained sample was analysed with HR-MS. Both characteristic signals of [**1** + H]$^+$ and [**1** + Na]$^+$ ions were observed. This implies that **FQNC** was successfully photodeprotected releasing fluoroquinolone **1**.

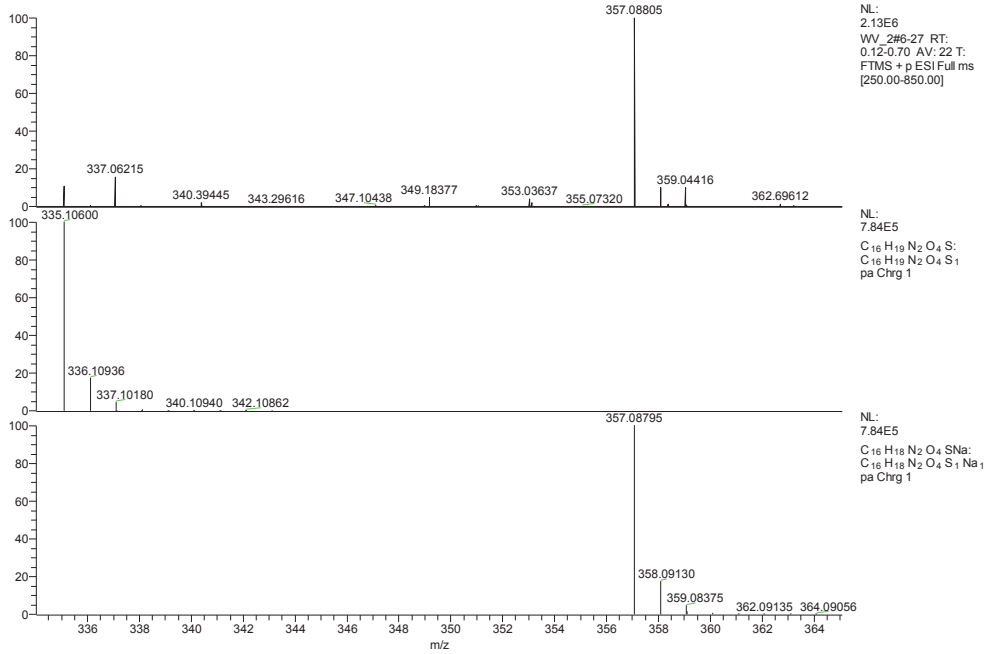

Figure S4 A saturated solution of **BPOC** in water was irradiated with 312 nm light for 2 min. The obtained sample was analysed with HR-MS. The characteristic signal of [**1** + Na]$^+$ ion was observed. This implies that **BPOC** was successfully photodeprotected releasing benzylpenicillin **2**.

Stability of FQNC and BPOC

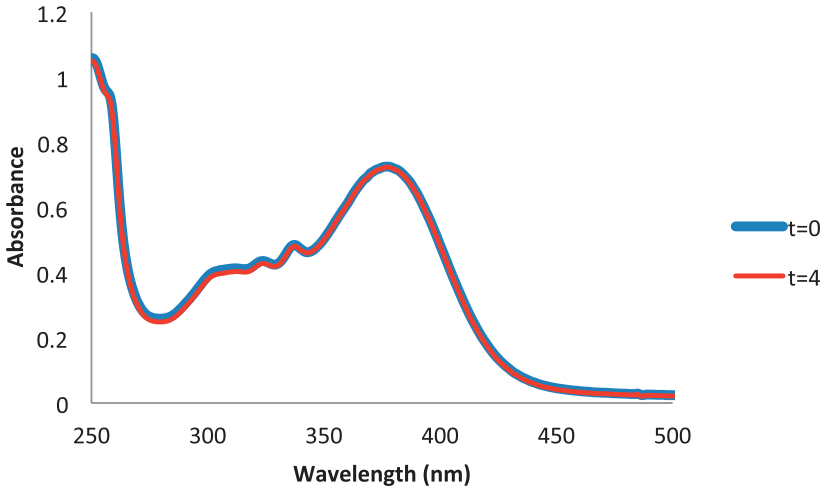

Figure S5 UV-Vis absorption spectra of a 38 μM solution of **FQNC** in water. After keeping the sample in the dark for 4 hours, no change in absorption spectrum could be observed, indicating that **FQNC** is stable for at least 4 hours in water.

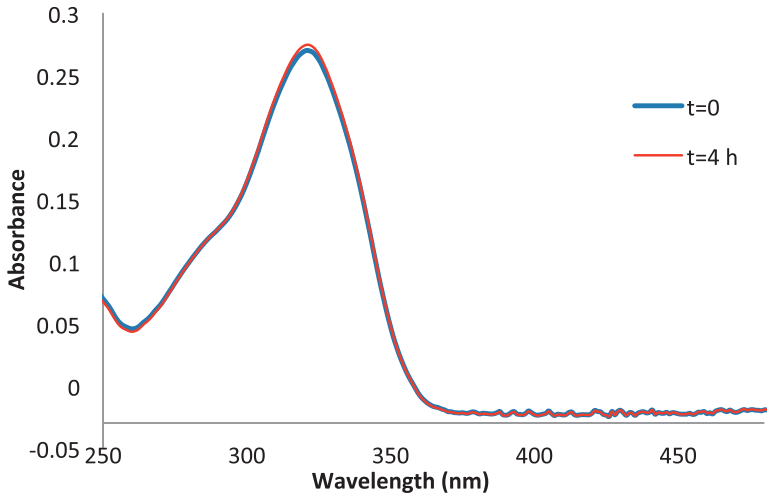

Figure S6 UV-Vis absorption spectra of a 14 μM solution of **BPOC** in water. After keeping the sample in the dark for 4 hours, no change in absorption spectrum could be observed, indicating that **BPOC** is stable for at least 4 hours in water.

MIC determination

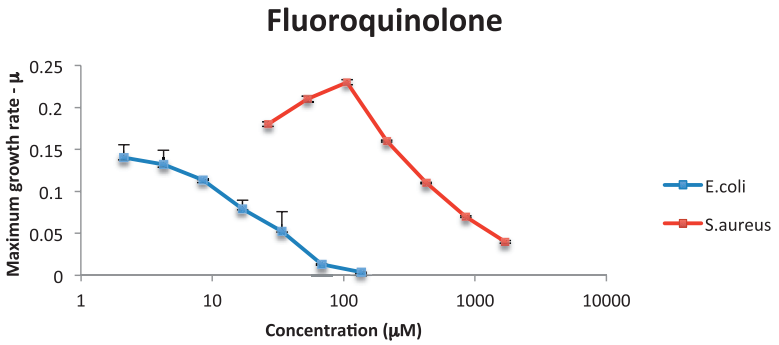

Figure S7 Growth rate of *E. coli* and *S. aureus* at different concentrations of fluoroquinolone.

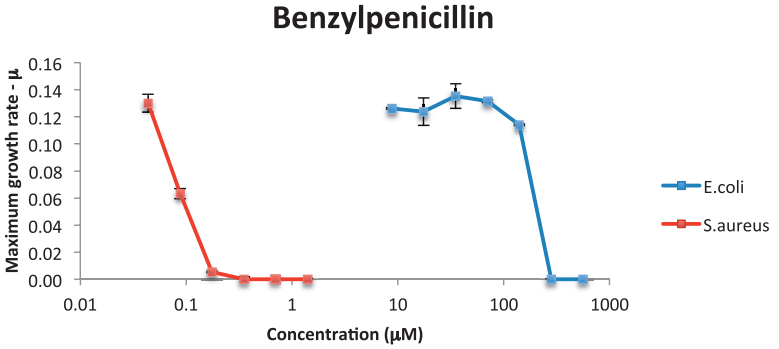

Figure S8 Growth rate of *E. coli* and *S. aureus* at different concentrations of benzylpenicillin.

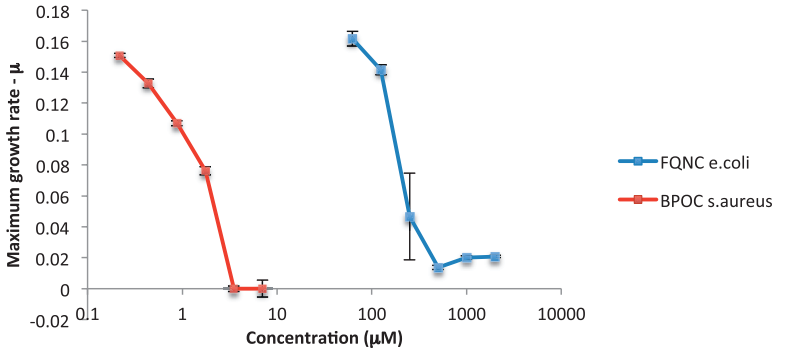

Figure S9 Growth rate of *E. coli* at different concentrations of **FQNC** (without light) and *S. aureus* at different concentrations of **BPOC** (without light).

Synthesis of FQNC and BPOC

Scheme 1 Synthesis of fluoroquinolone

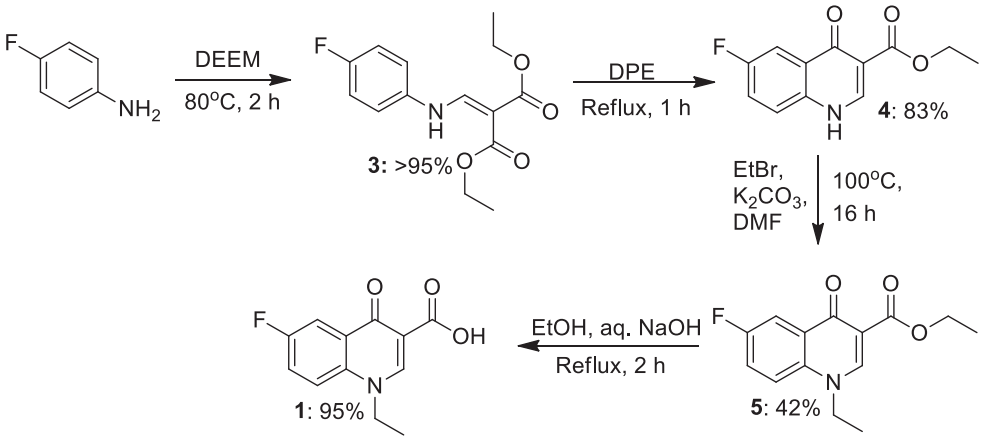

Scheme 2 Synthesis of **FQNC**

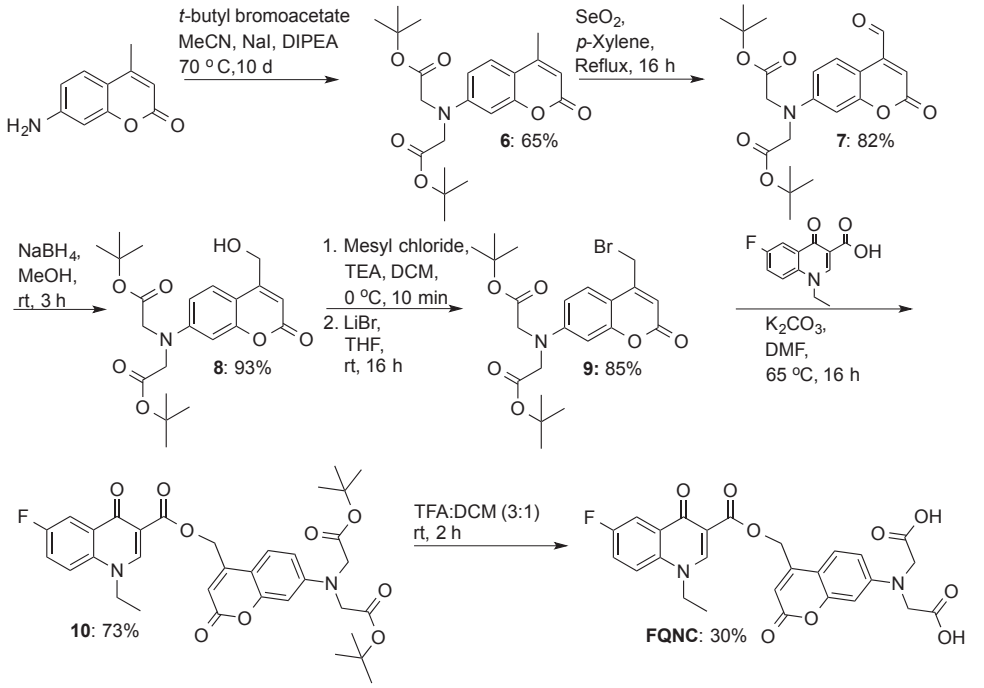

Scheme 3 Synthesis of **BPOC**

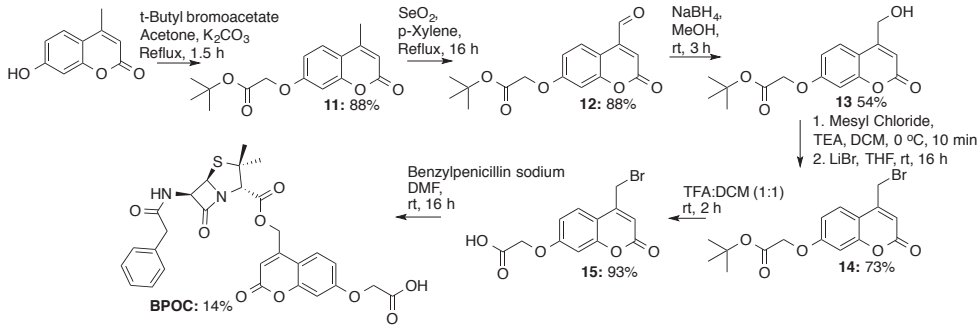

Experimental

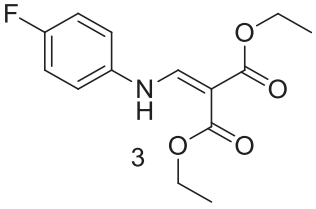

Diethyl 2-(((4-fluorophenyl)amino)methylene)malonate (**3**) A mixture of 4-fluoroaniline (18.0 mmol, 2.00 g) and diethyl-2-ethoxymethylenemalonate (DEEM) (18.0 mmol, 3.89 g) was stirred at 80 °C under a nitrogen atmosphere for 2 h. The reaction mixture was dissolved in DCM (50 mL), washed with aqueous 1M HCl (50 mL), brine (50 mL) and dried ($MgSO_4$). DCM was removed *in vacuo* resulting in 4.90 g (>95%) of a yellow solid.

^{1}H NMR (400 MHz, $CDCl_3$): δ 10.95 (d, *J* = 13.5 Hz, 1H), 8.39 (d, *J* = 13.9 Hz, 1H), 7.10 – 6.99 (m, 4H), 4.30 – 4.16 (m, 4H), 1.36-1.24 (m, 6H).

^{1}H NMR spectrum in agreement with published data [(4)].

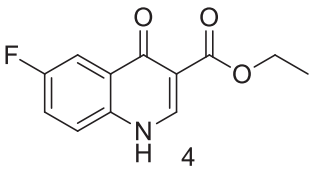

4

Ethyl 6-fluoro-4-oxo-1,4-dihydroquinoline-3-carboxylate (**4**) A solution of **3** (17.5 mmol, 4.90 g) in diphenylether (5 mL) was added dropwise to boiling diphenylether (60 mL). After heating under reflux for 1 h, the mixture was slowly cooled to room temperature and pentane (60 mL) was added. The solid was filtered off and the residue was recrystallized from DMF resulting in 3.40 g (83%) of a white solid.

^{1}H NMR (400 MHz, DMSO-D$_6$): δ 12.43 (s, 1H), 8.56 (s, 1H), 7.78 (dd, *J* = 9.3, 2.9 Hz, 1H), 7.69 (dd, *J* = 9.0, 4.6 Hz, 1H), 7.60 (td, *J* = 8.8, 3.0 Hz, 1H), 4.20 (q, *J* = 7.1 Hz, 2H), 1.26 (t, *J* = 7.1 Hz, 3H).

^{1}H NMR spectrum in agreement with published data [5].

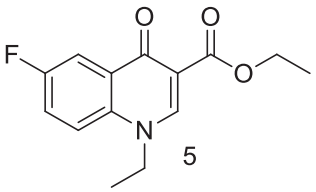

5

Ethyl 1-ethyl-6-fluoro-4-oxo-1,4-dihydroquinoline-3-carboxylate (**5**) To a solution of **4** (14.5 mmol, 3.40 g) in DMF (50 mL) was added K_2CO_3 (15.0 mmol, 2.07 g) and the resulting suspension was heated to 80 °C. Ethyl bromide (20 mmol, 2.16 g) was added and the mixture was stirred overnight. The mixture was diluted with water (100 ml) and filtered over a glass filter. The solid was recrystallized from EtOH resulting in 1.6 g (42%) of a white powder.

^{1}H NMR (400 MHz, DMSO-D$_6$): δ 8.69 (s, 1H), 7.90 (m, 2H), 7.68 (m, 1H), 4.41 (q, *J* = 7.1 Hz, 2H), 4.21 (q, *J* = 7.1 Hz, 2H), 1.35 (t, *J* = 7.1 Hz, 3H), 1.27 (t, *J* = 7.1 Hz, 3H).

^{1}H NMR spectrum in agreement with published data [5].

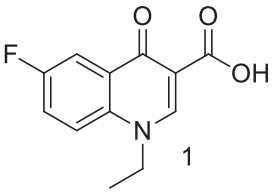

1-Ethyl-6-fluoro-4-oxo-1,4-dihydroquinoline-3-carboxylic acid (**1**) Compound **5** (0.38 mmol, 100 mg) was added to EtOH (5 mL) on ice and a 2.5 M aq. NaOH solution (152 µL) was added dropwise. The reaction mixture was heated at 70 °C for 16 h. Subsequently, aqueous 1 M HCl (5 mL) was added and the precipitate was filtered off resulting in 85 mg (95%) of a white solid.

^{1}H NMR (400 MHz, DMSO-D$_6$): δ 15.00 (s, 1H), 9.06 (s, 1H), 8.16 (dd, *J* = 9.4, 4.4 Hz, 1H), 8.04 (dd, *J* = 8.8, 3.1 Hz, 1H), 7.88 (ddd, *J* = 9.4, 8.0, 3.1 Hz, 1H), 4.61 (q, *J* = 7.2 Hz, 2H), 1.40 (t, *J* = 7.2 Hz, 3H).

^{1}H NMR spectrum in agreement with published data [5].

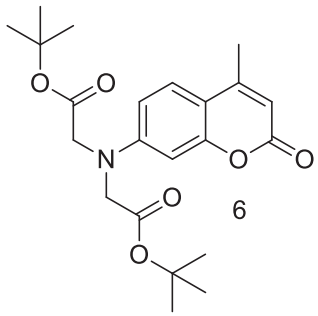

Di-tert-butyl 2,2'-((4-methyl-2-oxo-2H-chromen-7-yl)azanediyl)diacetate (**6**) A mixture of 7-amino-4-methylcoumarin (5.71 mmol, 1.00 g), *t*-butyl bromoacetate (57.1 mmol, 11.1 g), NaI (11.4 mmol, 1.71 g) and DIPEA (22.9 mmol, 2.95 g) in acetonitrile (60 mL) was heated at reflux for 10 d. The mixture was concentrated *in vacuo*. The residue was dissolved in EtOAc (50 mL), the solution was washed with water (50 mL) and brine (50 mL) and dried ($MgSO_4$). After purification by flash chromatography (pentane:EtOAc, 5:1, v/v), 1.50 g (65%) of an orange solid was obtained.

^{1}H NMR (400 MHz, CDCl$_3$): δ 7.42 (d, *J* = 8.9 Hz, 1H), 6.52 (dd, *J* = 8.9, 2.6 Hz, 1H), 6.45 (d, *J* = 2.6 Hz, 1H), 6.02 (d, *J* = 1.1 Hz, 1H), 4.05 (s, 4H), 2.35 (d, *J* = 1.1 Hz, 3H), 1.48 (d, *J* = 1.9 Hz, 18H).

^{1}H NMR spectrum in agreement with published data [6].

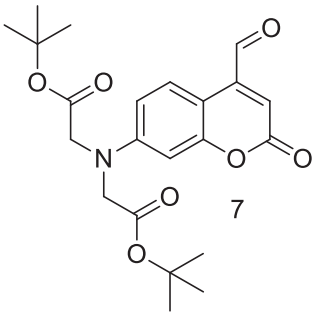

7

Di-tert-butyl 2,2'-((4-formyl-2-oxo-2H-chromen-7-yl)azanediyl)diacetate (**7**) Selenium dioxide (2.00 mmol, 220 mg) was added to a solution of compound **6** (1.00 mmol, 403 mg) in *p*-xylene (10 mL). The resulting mixture was heated at reflux for 16 h after which it was filtered while hot. The filtrate was concentrated *in vacuo* resulting in 343 mg (82%) of an orange solid.

^{1}H NMR (400 MHz, DMSO-D$_6$): δ 10.06 (s, 1H), 8.21 (d, *J* = 9.1 Hz, 1H), 6.74 (s, 1H), 6.63 (dd, *J* = 9.2, 2.7 Hz, 1H), 6.50 (d, *J* = 2.6 Hz, 1H), 4.18 (s, 4H), 1.40 (s, 18H).

^{1}H NMR spectrum in agreement with published data [7].

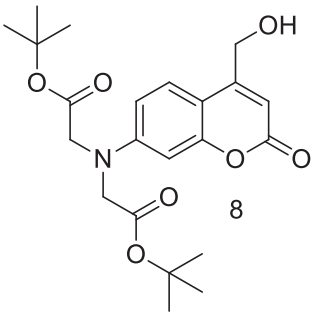

8

Di-tert-butyl 2,2'-((4-(hydroxymethyl)-2-oxo-2H-chromen-7-yl)azanediyl)diacetate (**8**) Compound **7** (0.36 mmol, 150 mg) was dissolved in methanol (10 mL) and the solution was cooled on ice. $NaBH_4$ (0.54 mmol, 21 mg) was added in small portions and the reaction mixture was stirred for 3 h. Next, the reaction was quenched by addition of 1 N aqueous HCl (10 mL) and the mixture extracted twice with EtOAc (20 mL). The combined organic layers were washed with brine (20 mL) and dried ($MgSO_4$). Concentrating *in vacuo* resulted in 140 mg (93%) of an orange solid.

^{1}H NMR (400 MHz, DMSO-D$_6$): δ 7.47 (d, *J* = 8.8 Hz, 1H), 6.52 (dd, *J* = 8.8, 2.5 Hz, 1H), 6.42 (d, *J* = 2.2 Hz, 1H), 6.13 (s, 1H), 5.52 (t, *J* = 5.5 Hz, 1H), 4.66 (d, *J* = 5.0 Hz, 2H), 4.16 (s, 4H), 1.40 (s, 18H).

^{1}H NMR spectrum in agreement with published data [7].

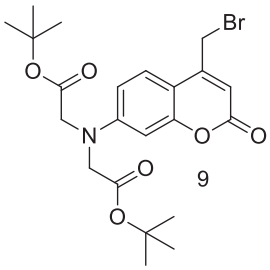

9

Di-tert-butyl 2,2'-((4-(bromomethyl)-2-oxo-2H-chromen-7-yl)azanediyl)diacetate (**9**) Compound **8** (0.33 mmol, 140 mg) was dissolved in DCM (5 mL) and the solution was cooled on ice. To this was slowly added TEA (0.66 mmol, 67 mg) and methanesulfonic acid chloride (0.49 mmol, 56 mg) and the resulting mixture was stirred for 30 min. Next, the reaction mixture was washed with a saturated aqueous $NaHCO_3$ solution (5 mL) and brine (5 mL) and dried ($MgSO_4$). After concentrating *in vacuo*, the resulting solid was dissolved in THF (5 mL) and LiBr (1.32 mmol, 115 mg) was added. The obtained solution was stirred for 16 h at room temperature after which it was concentrated *in vacuo*. Next, the solid was dissolved in DCM (10 mL) and the solution was washed with water (10 mL) and brine (10 mL) and dried ($MgSO_4$). After concentrating *in vacuo*, 135 mg (85%) of an orange solid was obtained.

^{1}H NMR (400 MHz, DMSO-D$_6$): δ 7.65 (d, *J* = 9.0 Hz, 1H), 6.61 (dd, *J* = 9.0, 2.7 Hz, 1H), 6.44 (d, *J* = 2.6 Hz, 1H), 6.34 (s, 1H), 4.78 (s, 2H), 4.18 (s, 3H), 1.40 (s, 18H).
^{1}H NMR spectrum in agreement with published data [7].

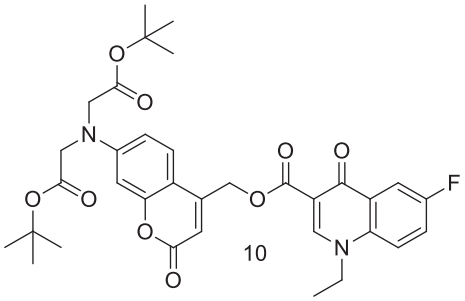

10

Di-tert-butyl 2,2'-((4-(((1-ethyl-6-fluoro-4-oxo-1,4-dihydroquinoline-3-carbonyl)oxy)methyl)-2-oxo-2H-chromen-7-yl)azanediyl)diacetate (**10**) Compound **9** (0.26 mmol, 123 mg) and compound (**1**) (0.26 mmol, 60 mg) were dissolved in DMF (2 mL) to which K_2CO_3 (0.38 mmol, 53 mg) was added. The reaction mixture was stirred for 16 h at 65 °C after which it was poured on cold water (10 mL). The resulting precipitate was filtered off and dried yielding 120 mg (73 %) of an orange solid.

^{1}H NMR (400 MHz, DMSO-D_6): δ 8.83 (s, 1H), 8.00 – 7.90 (m, 2H), 7.70 (d, *J* = 9.7 Hz, 1H), 7.60 (d, *J* = 8.9 Hz, 1H), 6.57 (d, *J* = 8.9 Hz, 1H), 6.53 (s, 1H), 6.47 (s, 1H), 5.51 (s, 2H), 4.46 (q, *J* = 7.2 Hz, 2H), 4.18 (s, 4H), 1.46 – 1.29 (m, 19H).
^{13}C NMR (100 MHz, DMSO-D_6): δ 169.3, 169.2, 164.9, 161.0, 158.5, 155.4, 151.7, 151.4, 150.2, 135.7, 130.7, 125.7, 120.9, 115.9, 113.7, 111.6, 111.4, 109.5, 108.7, 107.4, 106.9, 105.7, 98.5, 65.3, 55.3, 53.9, 48.8, 15.5, 14.8.
HR-MS (ESI, [M+H]$^+$): Calcd. for $C_{34}H_{38}FN_2O_9$: 637.2556; Found: 637.2550

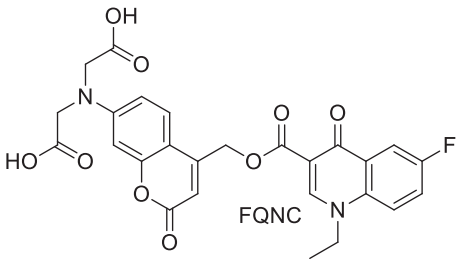

2,2'-((4-(((1-Ethyl-6-fluoro-4-oxo-1,4-dihydroquinoline-3-carbonyl)oxy)methyl)-2-oxo-2H-chromen-7-yl)azanediyl)diacetic acid (**FQNC**) Compound **10** (0.16 mmol, 100 mg) was dissolved in TFA:DCM (3:1) (4 mL) and the mixture stirred for 2 h at room temperature after which the solvents were evaporated. Diethylether (2 mL) was added to the obtained liquid which resulted in the formation of an orange precipitate. The solid was filtered off and recrystallized from MeOH to obtain 25 mg (30%) of an orange solid. Mp: 153-155 °C.
^{1}H NMR (400 MHz, DMSO-D_6): δ 8.84 (s, 1H), 7.96 (dd, *J* = 9.4, 5.6 Hz, 2H), 7.72 (m, 1H), 7.57 (d, *J* = 9.1 Hz, 1H), 6.60 (d, *J* = 8.7 Hz, 1H), 6.53 (s, 1H), 6.48 (s, 1H), 5.51 (s, 2H), 4.47 (q, *J* = 7.1Hz, 2H), 4.22 (s, 4H), 1.37 (t, *J* = 7.1 Hz, 3H).
^{13}C NMR (100 MHz, DMSO-D_6): δ 172.4, 171.8, 171.7, 164.9, 162.7, 161.0, 158.6, 155.4, 151.8, 151.4, 150.2, 135.7, 130.7, 125.7, 121.4, 120.9, 111.7, 111.5, 109.5, 108.7, 107.2, 98.4, 61.6, 53.1, 48.8, 14.8.
HR-MS (ESI, [M+H]$^+$): Calcd. for $C_{26}H_{22}O_9$: 525.1304; Found: 525.1294

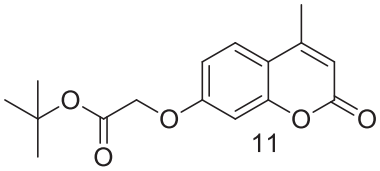

11

tert-butyl 2-((4-methyl-2-oxo-2H-chromen-7-yl)oxy)acetate (**11**) 7-Hydroxy-4-methylcoumarin (2.84 mmol, 500 mg) and *t*-butyl bromoacetate (3.7 mmol, 720 mg) were dissolved in acetone (10 mL) to which K_2CO_3 (4.26 mmol, 588 mg) was added. The reaction mixture was stirred while heated at reflux for 2 h, after which the solvent was evaporated. The white residue was dissolved in DCM (20 mL) and the solution was washed with water (2 x 20 mL) and brine (20 mL) and dried ($MgSO_4$). After concentrating *in vacuo*, 718 mg (88%) of a white solid was obtained.

^{1}H NMR (400 MHz, DMSO-D$_6$): δ 7.68 (d, *J* = 8.6 Hz, 1H), 6.97 – 6.91 (m, 2H), 6.21 (s, 1H), 4.79 (s, 2H), 2.38 (s, 3H), 1.42 (s, 9H).

^{13}C NMR (100 MHz, DMSO-D$_6$): δ 167.7, 161.1, 160.5, 154.9, 153.8, 126.9, 114.0, 112.6, 111.8, 101.9, 82.1, 65.6, 28.1, 18.5.

HR-MS (ESI, [M+H]$^+$): Calcd. for $C_{16}H_{19}O_5$: 291.1227; Found: 291.1216

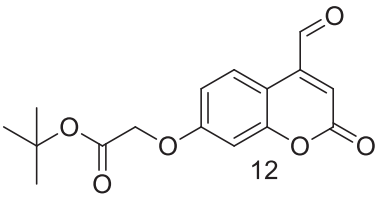

12

tert-butyl 2-((4-formyl-2-oxo-2H-chromen-7-yl)oxy)acetate (**12**) Selenium dioxide (3.45 mmol, 379 mg) was added to a solution of compound **11** (1.72 mmol, 500 mg) in *p*-xylene (10 mL). The resulting mixture was heated at reflux for 16 h after which it was filtered while hot. The filtrate was concentrated *in vacuo*, resulting in 460 mg (88%) of a white solid.

^{1}H NMR (400 MHz, DMSO-D$_6$): δ 10.09 (s, 1H), 8.38 (d, *J* = 8.6 Hz, 1H), 7.05 – 6.98 (m, 3H), 4.82 (s, 2H), 1.42 (s, 9H).

^{13}C NMR (100 MHz, DMSO-D$_6$): δ 194.0, 167.6, 161.3, 160.8, 156.0, 143.8, 127.4, 122.1, 113.4, 109.1, 102.3, 82.2, 65.6, 28.1.

HR-MS (ESI, [M+H]$^+$): Calcd. for $C_{16}H_{17}O_6$: 305.1019; Found: 305.1018

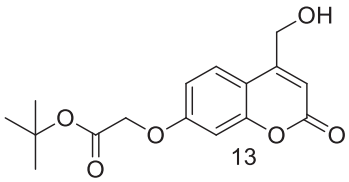

13

Di-tert-butyl 2,2'-((4-(hydroxymethyl)-2-oxo-2H-chromen-7-yl)azanediyl)diacetate (**13**) A solution of compound **12** (1.51 mmol, 460 mg) in methanol (10 mL) was cooled on ice. $NaBH_4$ (2.70 mmol, 86 mg) was added in small portions and the reaction mixture was stirred for 3 h. Next, the reaction was quenched by addition of aqueous 1 M HCl (10 mL) and the mixture was extracted twice with EtOAc (20 mL). The combined organic layers were washed with brine (20 mL) and dried ($MgSO_4$). Concentrating *in vacuo* resulted in 250 mg (54%) of a white solid.

^{1}H NMR (400 MHz, DMSO-D$_6$): δ 7.61 (d, *J* = 8.7 Hz, 1H), 6.97 – 6.89 (m, 2H), 6.30 (s, 1H), 5.60 (t, *J* = 4.4 Hz, 1H), 4.79 (s, 2H), 4.71 (d, *J* = 4.4 Hz, 2H), 1.42 (s, 9H).

^{13}C NMR (100 MHz, DMSO-D$_6$): δ 167.74, 160.9, 160.8, 157.0, 154.9, 125.8, 112.6, 111.6, 108.1, 102.0, 82.1, 65.6, 59.5, 28.2.

HR-MS (ESI, [M+H]$^+$): Calcd. for $C_{16}H_{19}O_6$: 307.1182; Found: 307.1165

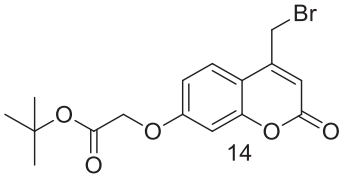

14

tert-butyl 2-((4-(bromomethyl)-2-oxo-2H-chromen-7-yl)oxy)acetate (**14**) A solution of compound **13** (0.69 mmol, 210 mg) in DCM (5 mL) was cooled on ice. To this was slowly added TEA (1.40 mmol, 141 mg) and methanesulfonic acid chloride (1.03 mmol, 118 mg) and the resulting mixture was stirred for 30 min. Next, the reaction mixture was washed with a saturated aqueous $NaHCO_3$ solution (5 mL) and brine (5 mL) and dried ($MgSO_4$). After concentrating *in vacuo*, the resulting solid was dissolved in THF (5 mL) and LiBr (2.76 mmol, 240 mg) was added. The obtained solution was stirred for 16 h at room temperature after which it was concentrated *in vacuo*. Next, the solid was dissolved in DCM (10 mL) and washed with water (10 mL) and brine (10 mL) and dried ($MgSO_4$). After concentrating in vacuo 186 mg (73%) of an orange solid was obtained.

^{1}H NMR (400 MHz, DMSO-D$_6$): δ 7.80 (d, *J* = 8.8 Hz, 1H), 7.04 – 6.95 (m, 2H), 6.55 (s, 1H), 4.84 (s, 2H), 4.81 (s, 2H), 1.42 (s, 9H).

^{13}C NMR (100 MHz, DMSO-D$_6$): δ 167.7, 161.4, 160.4, 155.5, 151.7, 127.0, 113.1, 112.8, 111.3, 102.3, 82.2, 65.6, 28.4, 28.1.

HR-MS (ESI, [M+H]$^+$): Calcd. for $C_{28}H_{27}N_2O_9S$: 369.0332; Found: 369.0331

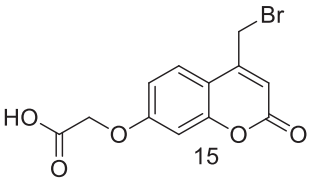

15

2-((4-Bromomethyl)-2-oxo-2H-chromen-7-yl)oxy)acetic acid (**15**) Compound **14** (0.82 mmol, 300 mg) was dissolved in TFA:DCM (1:1, v/v) (6 mL) and the solution was stirred for 2 h at room temperature, after which the volatiles were evaporated. Diethyl ether (2 mL) was added to the obtained liquid, which resulted in the formation of a white precipitate. The precipitate was filtered off, resulting in 240 mg (93%) of a white solid.

^{1}H NMR (400 MHz, DMSO-D$_6$): δ 7.75 (d, *J* = 8.7 Hz, 1H), 7.00-6.95 (m,2H), 6.51 (s, 1H), 4.81-4.78 (m, 4H).

^{13}C NMR (100 MHz, DMSO-D$_6$): δ 169.9, 161.4, 160.3, 155.5, 151.6, 126.9, 113.0, 112.8, 111.2, 102.2, 65.2, 28.4.

HR-MS (ESI, [M+H]$^+$): Calcd. for $C_{16}H_{17}BrO_5$: 312.9712; Found: 312.9707

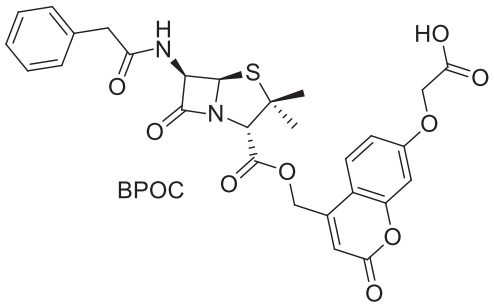

2-((4-((((2S,5R,6R)-3,3-dimethyl-7-oxo-6-(2-phenylacetamido)-4-thia-1-azabicyclo[3.2.0]heptane-2-carbonyl)oxy)methyl)-2-oxo-2H-chromen-7-yl)oxy)acetic acid (**BPOC**) A solution of compound **15** (0.32 mmol, 100 mg) and Penicillin G sodium salt (0.32 mmol, 114 mg) in DMF (5 mL) was stirred for 16 h at room temperature. Next, the solvent was evaporated and the crude product was recrystallized from MeOH and EtOAc, resulting in 25 mg (14%) of a white solid. Mp: 179-181 °C.

^{1}H NMR (400 MHz, DMSO-D$_6$): δ 8.90 (d, *J* = 6.6 Hz, 1H), 7.66 (d, *J* = 8.5 Hz, 1H), 7.29-7.15 (m, 5H), 7.01-6.95 (m, 2H), 6.42 (s, 1H), 5.54-5.39 (m, 4H), 4.82 (s, 2H), 4.64 (s, 1H), 3.57 – 3.47 (m, 2H) 1.60 (s, 3H), 1.42 (s, 3H).

^{13}C NMR (100 MHz, DMSO-D$_6$): δ 173.9, 170.8, 169.8, 167.4, 160.3, 155.2, 149.9, 136.3, 129.5, 128.7, 128.6, 126.9, 113.8, 113.1, 110.7, 110.1, 102.2, 70.2, 68.0, 64.6, 62.8, 59.3, 41.8, 36.2, 30.9, 27.0.

HR-MS (ESI, [M+H]$^+$): Calcd. for $C_{28}H_{27}N_2O_9S$: 567.1437; Found: 567.1420

References

1. Hatchard, C. G., and Parker, C. A. A New Sensitive Chemical Actinometer. II. Potassium Ferrioxalate as a Standard Chemical Actinometer. *Proc. R. Soc. London. Ser. A* **235**, 518–536 (1956).
2. Austin, E. A., Graves, J. F., Hite, L. A., Parker, C. T., and Schnaitman, C. A. Genetic analysis of lipopolysaccharide core biosynthesis by *Escherichia coli* K-12: insertion mutagenesis of the *rfa* locus. *J. Bacteriol.* **172**, 5312–5325 (1990).
3. Kreiswirth, B. N. *et al.* The toxic shock syndrome exotoxin structural gene is not detectably transmitted by a prophage. *Nature* **305**, 709–712 (1983).
4. Eswaran, S., Adhikari, A. V., Pal, N. K., and Chowdhury, I. H. Design and synthesis of some new quinoline-3-carbohydrazone derivatives as potential antimycobacterial agents. *Bioorganic Med. Chem. Lett.* **20**, 1040–1044 (2010).
5. Niedermeier, S. *et al.* A small-molecule inhibitor of Nipah virus envelope protein-mediated membrane fusion. *J. Med. Chem.* **52**, 4257–4265 (2009).
6. Noguchi, M. *et al.* Development of novel water-soluble photocleavable protective group and its application for design of photoresponsive paclitaxel prodrugs. *Bioorganic Med. Chem.* **16**, 5389–5397 (2008).
7. Hagen, V. *et al.* Coumarinylmethyl esters for ultrafast release of high concentrations of cyclic nucleotides upon one- and two-photon photolysis. *Angew. Chem. Int. Ed. Engl.* **44**, 7887–7891 (2005).